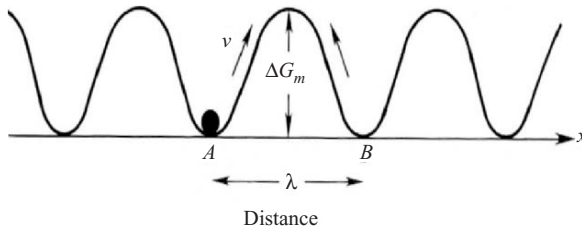

Appendix A: Diffusivity of Vacancy Mechanism of Diffusion in Solids

To analyze atomic diffusivity, we shall consider the vacancy mechanism of diffusion in a face-centered-cubic metal. We make the following assumptions in order to develop the analytical model.

1. It is a thermally activated unimolecular process. Unimolecular process means that we consider a single atom in the diffusion process and it is a near-equilibrium process. This is unlike chemical reactions that are bimolecular processes, such as rock salt formation, in which the collision of two atoms of Na and Cl is involved and the process is far from equilibrium.
2. It is a defect-mediated process. Here the defect is a vacancy.
3. The activated state obeys a Boltzmann's equilibrium distribution from transition state theory. Hence, the Boltzmann distribution function is used.
4. It is assumed that the probability of reverse jumps is large due to small driving force, so we have to consider reverse processes. In other words, the process is not far from equilibrium.
5. Statistically, atomic diffusion obeys the principle of random walk.
6. A long-range diffusion requires a driving force.



At equilibrium, in a one-dimensional configuration, atoms are attempting to jump over the potential energy barrier with the attempt frequency, ν_0 , to exchange position with a neighboring vacancy, as depicted in Fig. A.1.

The successful or exchange jump frequency is given below on the basis of Boltzmann's distribution:

$$\nu = \nu_0 \exp\left(\frac{-\Delta G_m}{kT}\right),$$

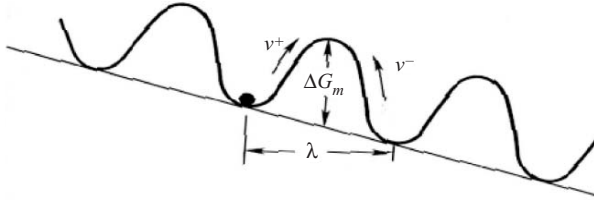
where

ν_0 = attempt frequency,

ν = exchange frequency,

ΔG_m = saddle point energy (activation energy of motion).

We note that there is a reverse jump at the same attempt frequency.



Now consider a driving force F (which equals the slope of the base line in Fig. A.2). The meaning of F will be discussed later. The forward jump is increased by

$$\nu^+ = \nu \exp\left(+\frac{\lambda F}{2kT}\right),$$

where λ is the jump distance. The reverse jump is decreased by

$$\nu^- = \nu \exp\left(-\frac{\lambda F}{2kT}\right).$$

And the net frequency is

$$\nu_n = \nu^+ - \nu^- = 2\nu \sinh\left(\frac{\lambda F}{2kT}\right).$$

Now, we take the "condition of linearization,"

$$\frac{\lambda F}{kT} \ll 1.$$

Then the net frequency jump v_n is “linearly” proportional to the driving force F :

$$v_n = v \frac{\lambda F}{kT}.$$

We can define a drift velocity

$$v = \lambda v_n = \frac{v\lambda^2}{kT} F.$$

Then, the atomic flux J , which has units of number of atoms per unit area per unit time, is

$$J = Cv = \frac{Cv\lambda^2}{kT} F,$$

where $M = v\lambda^2/kT$ is defined as the atomic mobility. The atomic flux J is “linearly” proportional to the driving force F . The driving force is generally defined as a potential gradient,

$$F = -\frac{\partial\mu}{\partial x}.$$

In atomic diffusion, here μ is the chemical potential of an atom and is defined at constant temperature and pressure to be

$$\mu = \left(\frac{\partial G}{\partial C} \right)_{T,p},$$

where G is Gibbs free energy and C is concentration. For an ideal dilute solid solution,

$$\begin{aligned} \mu &= kT \ln C, \\ F &= -\frac{\partial\mu}{\partial C} \frac{\partial C}{\partial x} = -\frac{kT}{C} \frac{\partial C}{\partial x}, \\ J &= \frac{Cv\lambda^2}{kT} F = \frac{Cv\lambda^2}{kT} \left(-\frac{kT}{C} \frac{\partial C}{\partial x} \right) = -v\lambda^2 \left(\frac{\partial C}{\partial x} \right) = -D \left(\frac{\partial C}{\partial x} \right). \end{aligned}$$

Hence, we have obtained Fick’s first law of diffusion:

$$\frac{J}{-\left(\frac{\partial C}{\partial x}\right)} = D = v\lambda^2,$$

where D is the diffusion coefficient (or diffusivity) in units of cm^2/sec . Then, $M = D/kT$. In the above derivation, as depicted in Fig. A.1, we have assumed

that the diffusing atom has a neighboring vacancy. For the majority of atoms in the lattice, this is not true, and we must define the probability of an atom having a neighboring vacancy in the solid as

$$\frac{n_v}{n} = \exp\left(-\frac{\Delta G_f}{kT}\right).$$

n_v is the total number of vacancies in the solid, n is the total number of lattice sites in the solid, and ΔG_f is the Gibbs free energy of formation of a vacancy. Since in a face-centered-cubic metal, a lattice atom has 12 nearest neighbors, the probability of a particular atom having a vacancy as a neighbor is

$$n_c \frac{n_v}{n} = n_c \exp\left(-\frac{\Delta G_f}{kT}\right) \quad n_c = 12.$$

Next, we have to consider the correlation factor in the face-centered-cubic lattice. The physical meaning of the factor is the probability of reverse jump; after the atom has exchanged position with a vacancy, it has a high probability of returning to its original position before the activated configuration is relaxed. The factor has a range between zero and unity. When $f = 0$, it means the probability of reverse jump is 100%, so the atom and the vacancy are exchanging position back and forth, which will not lead to any random walk but instead a correlated walk. When $f = 1$, it means that after the jump, the atom will not return to its original position, and it is a random walk because the next jump will depend on the random probability of a vacancy coming to the neighborhood of this atom. In fcc metals, $f = 0.78$, so about 80% of jumps are random walk, and about 20% are correlated walk. Finally, we have the diffusivity as

$$D = f n_c a^2 \nu_0 \exp\left(-\frac{\Delta G_m + \Delta G_f}{kT}\right),$$

$$D = f n_c \lambda^2 \nu_0 \exp\left(\frac{\Delta S_m + \Delta S_f}{k}\right) \exp\left(-\frac{\Delta H_m + \Delta H_f}{kT}\right) = D_0 \exp\left[-\frac{\Delta H}{kT}\right].$$

Appendix B: Growth and Ripening Equations of Precipitates

The distribution function of a set of precipitates is obtained by solving the continuity equation in size space:

$$\frac{\partial f}{\partial t} = v \frac{\partial f}{\partial x},$$

where f is the size distribution function of the precipitates and v is the growth/dissolution velocity of the precipitates. To solve the continuity equation, the first step is to find the growth/dissolution velocity. In this appendix we shall derive the velocity of a spherical precipitate. When the diameter of the precipitates is in nanoscale, it is important to take into account the Gibbs–Thomson potential of curvature as in the LSW theory of ripening. In other words, the equilibrium concentration at the precipitate/matrix interface is a function of radius. When the precipitate diameter is large, we can assume the equilibrium concentration to be constant, independent of the radius.

B.1 Kinetics of Precipitation

We consider the growth or dissolution of a spherical particle or precipitate. Letting R be the variable, the diffusion equation in spherical coordination, assuming a steady state, is

$$\frac{\partial^2 C}{\partial R^2} + \frac{2}{R} \frac{\partial C}{\partial R} = 0.$$

The solution is

$$C = \frac{b}{R} + d. \tag{B.1}$$

The boundary conditions are

$$\text{At } R = r_0, C = C_0, \quad \text{we have } C_0 = \frac{b}{r_0} + d. \quad (\text{B.2})$$

$$\text{At } R = r, C = C_r, \quad \text{we have } C_r = \frac{b}{r} + d. \quad (\text{B.3})$$

Now, if we take the difference between the last two equations, we have

$$C_r - C_0 = b \left(\frac{1}{r} - \frac{1}{r_0} \right) = b \frac{r_0 - r}{rr_0} \cong \frac{b}{r} \quad \text{where } r_0 \gg r. \quad (\text{B.4})$$

This is an important assumption. It means that precipitates are far apart. Note that if we take the volume fraction, f , the ratio of volume of the precipitate particles to the volume of the diffusion field, or the total volume of the precipitated phase to the total volume of the matrix, is

$$f = \frac{\frac{4\pi}{3}r^3}{\frac{4\pi}{3}r_0^3} = \frac{r^3}{r_0^3} \rightarrow 0.$$

It is a very small value: $f \rightarrow 0$. (This is a very important assumption in the LSW theory of ripening to be discussed later.)

We have $b = r(C_r - C_0)$. Substituting b into Eq. (B.3), we have

$$C_r = \frac{r(C_r - C_0)}{r} + d. \quad (\text{B.5})$$

We have $d = C_0$, and Eq. (B.1) becomes

$$C(R) = \frac{(C_r - C_0)r}{R} + C_0. \quad (\text{B.6})$$

Therefore,
$$\frac{dC}{dR} = -\frac{(C_r - C_0)r}{R^2}.$$

At the particle/matrix interface for a particle of radius r , or $R = r$, we have

$$\frac{dC}{dR} = -\frac{C_r - C_0}{r}. \quad (\text{B.7})$$

Then the flux of atoms arriving at the interface is

$$J = +D \frac{\partial C}{\partial R} = \frac{D(C_0 - C_r)}{r} \quad \text{at } R = r. \quad (\text{B.8})$$

Note that when $C_r > C_0$, $J < 0$, the net flux is toward the particle, and thus

it grows. When $C_r < C_0$, $J > 0$, the flux leaves the particle so the particle dissolves.

B.2 Growth Rate of a Spherical Particle Assuming C_r Is Constant

If Ω is atomic volume, in time dt , a volume is added to the spherical particle,

$$\Omega J A dt = \Omega J 4\pi r^2 dt = 4\pi r^2 dr,$$

where the last term is the increment of a spherical shell due to the growth. Hence,

$$\frac{dr}{dt} = \Omega J = \frac{\Omega D(C_0 - C_r)}{r}. \quad (\text{B.9})$$

B.2.1 Case 1: The Growth of a Precipitate

By integration and assuming when $t = 0$, $r = 0$,

$$r^2 = 2\Omega D(C_0 - C_r)t. \quad (\text{B.10})$$

Note here that if we follow Ham's approach and take C_r as a constant, it is not a function of r as given by the Gibbs–Thomson equation. From the above equation, we see that $r \cong t^{1/2}$ and $r^3 \cong t^{3/2}$. Or we have

$$r^3 = [2\Omega D(C_0 - C_r)t]^{3/2}. \quad (\text{B.11})$$

B.2.2 Case 2: The Depletion of Concentration in the Matrix (Mean-Field Consideration)

On the other hand, we consider the loss of average concentration in the matrix, $\Delta\bar{C} = C_0 - \bar{C}$, due to the formation of the precipitate, where the average concentration in the matrix is \bar{C} , which can be regarded as the “mean-field” concentration (the conception of mean-field theory). In the beginning, the average concentration is C_0 , and it changes to \bar{C} when the precipitate grows.

Let $1/\Omega = C_p$ be the concentration in the solid precipitate. We have simply by mass balance,

$$\frac{4\pi}{3} r_0^3 (C_0 - \bar{C}) = \frac{4\pi}{3} r^3 \frac{1}{\Omega} = \frac{4\pi}{3\Omega} [2\Omega D(C_0 - C_r)t]^{3/2}, \quad (\text{B.12})$$

$$\bar{C} = C_0 - \left[\frac{2D(C_0 - C_r)\Omega^{1/3}}{r_0^2} t \right]^{3/2} = C_0 - \left[\frac{2Bt}{3} \right]^{3/2}, \quad (\text{B.13})$$

where

$$B \equiv \frac{3D(C_0 - C_r)}{C_p^{1/3} r_0^2}.$$

We note that the above equation is the same as Eq. (1-36) in Chapter 1 in Shewmon.

B.2.3 Case 3: Consider Growth of Precipitate and Depletion of the Matrix Together

We can derive the last equation in a slightly different way. The growth of the precipitate reduces the concentration in the matrix. The amount of solute atoms diffusing to the precipitate in time Δt is

$$J(r)4\pi r^2 \Delta t = \text{number of atoms.}$$

It should be equal to the reduction of the average concentration in the volume of the sphere of diffusion of r_0 . Hence, if take the average concentration in the matrix to be \bar{C} ,

$$\frac{4\pi r_0^3}{3} \Delta \bar{C} = J(r)4\pi r^2 \Delta t.$$

Or, we have

$$\frac{\Delta \bar{C}}{\Delta t} = \frac{3}{4\pi r_0^3} 4\pi r^2 J(r) = -\frac{3D}{r_0^3} (C_0 - C_r)r. \quad (\text{B.14})$$

The conservation of mass requires that

$$\frac{4\pi}{3} r_0^3 (C_0 - \bar{C}) = \frac{4\pi}{3} r^3 C_p, \quad (\text{B.15})$$

where C_p is the concentration of solute in the solid precipitate and $C_p = 1/\Omega$. Hence,

$$r = r_0 \left(\frac{C_0 - \bar{C}}{C_p} \right)^{1/3}. \quad (\text{B.16})$$

By substituting r into the rate equation above, we have

$$\frac{\Delta \bar{C}}{\Delta t} = -\frac{3D}{r_0^2} (C_0 - C_r) \frac{1}{C_p^{1/3}} (C_0 - \bar{C})^{1/3}. \quad (\text{B.17})$$

Let

$$B \equiv \frac{3D(C_0 - C_r)}{C_p^{1/3} r_0^2}.$$

We have

$$\frac{d\bar{C}}{dt} = -B(C_0 - \bar{C})^{1/3}.$$

By integration we obtain

$$-\frac{3}{2}(C_0 - \bar{C})^{2/3} = -Bt + \beta.$$

At $t = 0, C_0 = \bar{C}$, so $\beta = 0$.

Thus, we have the solution,

$$\bar{C} = C_0 - \left(\frac{2Bt}{3}\right)^{3/2}, \quad (\text{B.18})$$

which is the same as what we have obtained. Hence, we have

$$C_0 - \bar{C} \cong t^{3/2} \text{ for 3-dimensional growth.}$$

$$\text{Let } \bar{C} = C_0 \left[1 - \left(\frac{2Bt}{3C_0^{2/3}} \right)^{3/2} \right] = C_0 \left[1 - \left(\frac{t}{\tau} \right)^{3/2} \right] = C_0 \exp \left[- \left(\frac{t}{\tau} \right)^{3/2} \right] \quad (\text{B.19})$$

if we assume $t \ll \tau$,

$$\text{where } \tau = \frac{C_p^{1/3} r_0^2 C_0^{2/3}}{2D(C_0 - C_r)} \cong \frac{r_0^2}{2D} \left(\frac{C_p}{C_0} \right)^{1/3}. \quad (\text{B.20})$$

Usually D, C_p, C_0 are known, and we can design the experiment to control the growth of the precipitate.

B.3 Gibbs–Thomson Potential: Effect of Surface Curvature

Consider a sphere with radius r and surface energy per unit area γ . The surface energy exerts a compressive pressure on the sphere because it tends

to shrink to reduce the surface energy. The pressure is

$$p = \frac{F}{A} = \frac{-\frac{dE}{dr}}{A} = \frac{-\frac{d4\pi r^2\gamma}{dr}}{4\pi r^2} = -\frac{8\pi r\gamma}{4\pi r^2} = -\frac{2\gamma}{r}. \quad (\text{B.21})$$

If we multiply p by the atomic volume Ω , we have the chemical potential

$$\mu_r = -\frac{2\gamma\Omega}{r}. \quad (\text{B.22})$$

This is called the Gibbs–Thomson potential due to the curvature of surface. We note that it is not just the potential of the surface atoms of the precipitate, it is the potential energy of all the atoms in the precipitate. We see that for a flat surface $r = \infty$, $\mu_\infty = 0$ so we have

$$u_r - \mu_\infty = \frac{2\gamma\Omega}{r}. \quad (\text{B.23})$$

In the following, we shall apply this potential to determine the effect of curvature on solubility. We consider an alloy of $\alpha = \text{A}(\text{B})$, where B is solute in solvent A. At temperature T, B will precipitate out. We consider two precipitates of B, one larger than the other. The solubility of B surrounding the large one is less than that surrounding the smaller one. If we take X to be the solubility, we have

$$X_\infty < X_{\text{large}} < X_{\text{small}}.$$

To relate the solubility to Gibbs–Thomson potential, we have the chemical potential of B as a function of its radius as

$$\mu_{\text{B},r} - \mu_{\text{B},\infty} = \frac{2\gamma\Omega}{r}, \quad (\text{B.24})$$

where γ is the interfacial energy between the precipitate and the matrix. If we define the standard state of B as pure B with $r = \infty$, we have

$$\mu_{\text{B},r} = \mu_{\text{B},\infty} + RT \ln a_{\text{B}}, \quad (\text{B.25})$$

where a_{B} is the activity. According to Henry's law,

$$a_{\text{B}} = kX_{\text{B},r},$$

where $X_{\text{B},r}$ is the solubility of B surrounding a precipitate of radius r . At $r = \infty$,

$$\mu_{\text{B},\infty} = \mu_{\text{B},\infty} + RT \ln a_{\text{B}}.$$

This implies that $RT \ln a_B = 0$, or $a_B = 1$. So $k = 1/X_{B,\infty}$. Therefore,

$$\mu_{B,r} = \mu_{B,\infty} + RT \ln \frac{X_{B,r}}{X_{B,\infty}}. \quad (\text{B.26})$$

Hence,

$$\ln \frac{X_{B,r}}{X_{B,\infty}} = \frac{\mu_{B,r} - \mu_{B,\infty}}{RT} = \frac{2\gamma\Omega}{rRT}.$$

Or if we consider kT instead of RT , we have

$$X_{B,r} = X_{B,\infty} \exp\left(\frac{2\gamma\Omega}{rkT}\right). \quad (\text{B.27})$$

B.4 Effect of Curvature on Solubility (Ripening)

The solubility of B around a spherical particle of B of radius r is given by

$$X_{B,r} = X_{B,\infty} \exp\left(\frac{2\gamma\Omega}{rkT}\right),$$

where $r = \infty$, the exponential equals unity. Thus, $X_{B,r}$ goes up when r goes down. Now we replace $X_{B,r}$ by C_r and $X_{B,\infty}$ by C_∞ , which is the equilibrium concentration on a flat surface. We have

$$C_r = C_\infty \exp\left(\frac{2\gamma\Omega}{rkT}\right). \quad (\text{B.28})$$

If $2\gamma\Omega \ll rkT$, we have

$$\begin{aligned} C_r &= C_\infty \left(1 + \frac{2\gamma\Omega}{rkT}\right), \\ C_r - C_\infty &= \frac{2\gamma\Omega C_\infty}{rkT} = \frac{\alpha}{r}, \end{aligned} \quad (\text{B.29})$$

where $\alpha = \frac{2\gamma\Omega}{kT} C_\infty$,

$$C_r = C_\infty + \frac{\alpha}{r}. \quad (\text{B.30})$$

Thus, C_r is not a constant, but a function of r . Now we substitute C_r into the growth equation of

$$\frac{dr}{dt} = \Omega J = \frac{\Omega D(C_0 - C_r)}{r}.$$

We have

$$\frac{dr}{dt} = \frac{\Omega D}{r} \left(C_0 - C_\infty - \frac{\alpha}{r} \right). \quad (\text{B.31})$$

Note that $C_0 - C_\infty > 0$ always. We can define a critical radius r^* such that

$$C_0 - C_\infty = \frac{\alpha}{r^*}.$$

Then we have

$$\frac{dr}{dt} = \frac{\alpha \Omega D}{r} \left(\frac{1}{r^*} - \frac{1}{r} \right). \quad (\text{B.32})$$

The parameter r^* is defined such that

- $r > r^*, \frac{dr}{dt} > 0$ The particle is growing.
- $r < r^*, \frac{dr}{dt} < 0$ The particle is dissolving.
- $r = r^*, \frac{dr}{dt} = 0$ The particle is in a state of metastable equilibrium. It has a concentration \bar{C} at the interface, or $C_{r^*} = \bar{C}$.

In ripening, the larger particles grow at the expense of the smaller ones. It will approach a dynamic equilibrium distribution of size of the particles. The distribution function can be obtained by solving the continuity equation in size space. Knowing dr/dt , it is the beginning of the LSW theory of ripening.

Appendix C: Derivation of Huntington's Electron Wind Force

In the following we present the assumptions and step-by-step derivation of Huntington's model of electron wind force.

(1) Considerations are semiclassical. Each electron is treated as a group of waves or Bloch waves with an average wave vector k and group velocity of $\bar{V} = \frac{1}{\hbar} \frac{\partial E(\bar{k})}{\partial \bar{k}}$, where the function $E(\bar{k})$ should be found from the electron band theory (dispersion law). For free electrons, $E(\bar{k}) = \frac{\hbar^2 k^2}{2m^*}$, and for electrons at the bottom of the conduction band, $E(\bar{k}) = E_{\min} + \frac{\hbar^2 k^2}{2m_0}$, where $m^* = \hbar^2 (\frac{\partial^2 E}{\partial k^2})^{-1}$ is the effective electron mass. We note that $\frac{\partial E}{\partial k}$ means gradient in k -space, e.g., a vector with components of $\frac{\partial E}{\partial k_x}, \frac{\partial E}{\partial k_y}, \frac{\partial E}{\partial k_z}$. For Bloch waves, according to the Bloch theorem, we recall that each quantum state of independent electron in the periodic potential $U(\bar{r} + \bar{R}) = U(\bar{r})$ and $\bar{R} = n_1 \bar{a}_1 + n_2 \bar{a}_2 + n_3 \bar{a}_3$ can be described by the product of a planar wave and periodic function $\Psi_{\bar{n}\bar{k}}(\bar{r}) = e^{i\bar{k}\bar{r}} W_{\bar{n}\bar{k}}(\bar{r})$, where $W_{\bar{n}\bar{k}}(\bar{r} + \bar{R}) = W_{\bar{n}\bar{k}}(\bar{r})$ and n is the band index.

(2) $\frac{1}{\hbar} (\frac{\partial E}{\partial k'} - \frac{\partial E}{\partial k}) = \bar{V}' - \bar{V}$ is the change of electron's group velocity as a result of scattering.

(3) $-\frac{m_0}{\hbar} (\frac{\partial E}{\partial k'_x} - \frac{\partial E}{\partial k_x}) = -(p'_x - p_x)$ is momentum along the x -axis, transfer to defect during mentioned individual scattering.

(4) $f(\bar{k})$ is the probability that the quantum state \bar{k} is occupied by some electron. The quantum cell in k -space with a " k -volume" is given by $\Omega = \frac{2\bar{\mu}}{L_x} \cdot \frac{2\bar{\mu}}{L_y} \cdot \frac{2\bar{\mu}}{L_z} = \frac{8\pi^3}{V}$, where V is the real total volume. At equilibrium, we have $f_0 = \frac{1}{e^{\frac{E - \bar{\mu}}{\hbar kT}} + 1}$ (Fermi-Dirac distribution).

(5) $1 - f(\bar{k}')$ is a probability that the quantum state \bar{k}' was free or unoccupied before scattering, so that the Pauli exclusion principle does not forbid the $\bar{k} \rightarrow \bar{k}'$ transition.

(6) $W_d(\bar{k} \rightarrow \bar{k}')$ is a probability of this transition per unit time. It means that the product $W_d dt$ is a probability of transition during dt , if $dt \ll \tau_d$.

(7) According to the Pauli principle, each quantum cell in k -space (with $\Omega = \frac{8\pi^3}{V}$) may contain up to two electrons with opposite spins, so the k -volume per electron is $\frac{\Omega}{2} = \frac{4\pi^3}{V}$.

(8) Now we consider unit volume $V = 1 \text{ m}^3$.

(9) The number of possible electron states in the “elementary” k -volume $d_k^3 = dk_x dk_y dk_z$ is $\frac{d_k^3 \Omega}{2} = \frac{d_k^3 k}{4\pi^3}$. The elementary k -volume is physically small.

(10) The momentum, M_x along the x -axis, transferring from electrons to the defects in the unit volume $V = 1 \text{ m}^3$ per unit time is given as

$$- \iint \frac{d^3 k}{4\pi^3} \frac{d^3 k'}{4\pi^3} (p'_x - p_x) f(\bar{k})(1 - f(\bar{k}')) W_d(\bar{k}, \bar{k}').$$

Or

$$\frac{dM_x}{dt} = - \left(\frac{1}{4\pi^3} \right)^2 \iint \frac{m_0}{\hbar} \left(\frac{\partial E}{\partial k'_x} - \frac{\partial E}{\partial k_x} \right) f(\bar{k})(1 - f(\bar{k}')) W_d(\bar{k}, \bar{k}') d^3 k' d^3 k.$$

(11) We shall represent the last equation by two integrals.

$$\frac{dM_x}{dt} = I_1 + I_2,$$

where

$$I_1 = - \left(\frac{1}{4\pi^3} \right)^2 \iint \frac{m_0}{\hbar} \frac{\partial E}{\partial k'_x} f(\bar{k})(1 - f(\bar{k}')) W_d(\bar{k}, \bar{k}') d^3 k' d^3 k,$$

$$I_2 = - \left(\frac{1}{4\pi^3} \right)^2 \iint \frac{m_0}{\hbar} \frac{\partial E}{\partial k_x} f(\bar{k})(1 - f(\bar{k}')) W_d(\bar{k}, \bar{k}') d^3 k' d^3 k.$$

Since the integration is being made over all \bar{k} and all \bar{k}' , we can interchange the variables in the first integral as

$$I_1 = - \left(\frac{1}{4\pi^3} \right)^2 \iint \frac{m_0}{\hbar} \frac{\partial E}{\partial k_x} f(\bar{k}') (1 - f(\bar{k})) W_d(\bar{k}', \bar{k}) d^3 k' d^3 k.$$

Then in I_1 and I_2 , we have the same $\frac{\partial E}{\partial k_x}$, and thus we have

$$\frac{dM_x}{dt} = (-I_2) - (-I_1) \tag{C.1}$$

$$= \left(\frac{1}{4\pi^3} \right)^2 \iint \frac{m_0}{\hbar} \frac{\partial E}{\partial k_x} [f(\bar{k}') (1 - f(\bar{k})) W_d(\bar{k}, \bar{k}) - f(\bar{k}') (1 - f(\bar{k})) W_d(\bar{k}', \bar{k})] d^3 k' d^3 k.$$

(12) Huntington showed that to simplify the expression of the last equation, he used the concept of relaxation time τ_d . This notion was first introduced for the analysis of the kinetic Boltzmann equation for gases. With certain approximation, the rate of change of the distribution function can be represented as

$$\begin{aligned} \frac{\partial f(t, \bar{k})}{\partial t} = & \frac{1}{4\pi^3} \int \{f(\bar{k})(1 - f(\bar{k}'))W_d(\bar{k}, \bar{k}') \\ & - f(\bar{k}') (1 - f(\bar{k}))W_d(\bar{k}', \bar{k})\} d^3 k' - \frac{f(t, \bar{k}) - f(\bar{k})}{\tau_d} \end{aligned}$$

for the equilibrium distribution. For the stationary case, $\frac{\partial f}{\partial t} = 0$, so that

$$\begin{aligned} \frac{1}{4\pi^3} \int \{f(\bar{k})(1 - f(\bar{k}'))W_d(\bar{k}, \bar{k}') - f(\bar{k}') (1 - f(\bar{k}))W_d(\bar{k}', \bar{k})\} d^3 k' \\ = \frac{f(t, \bar{k}) - f(\bar{k})}{\tau_d}. \end{aligned} \quad (\text{C.2})$$

In the above equation, $f(\bar{k})(1 - f(\bar{k}'))W_d(\bar{k}, \bar{k}')$ is the probability per unit time of $\bar{k} \rightarrow \bar{k}'$ transition, provided that the state \bar{k} before transition was filled and the state \bar{k}' was empty. The function $f(\bar{k}') (1 - f(\bar{k}))W_d(\bar{k}', \bar{k})$ is the probability per unit time of the inverse transition.

(13) By substituting Eq. (C.2) into Eq. (C.1), we have

$$\frac{dM_x}{dt} = \frac{1}{4\pi^3} \int d^3 k \frac{m_0}{\hbar} \frac{\partial E(\bar{k})}{\partial k_x} \frac{f(\bar{k}) - f_0(\bar{k})}{\tau_d}.$$

(14) Let the relaxation time be independent of \bar{k} and $\tau_d = \text{constant}$. Then

$$\frac{dM_x}{dt} = \frac{m_0}{\hbar \tau_d} \frac{1}{4\pi^3} \int d^3 k \frac{\partial E(\bar{k})}{\partial k_x} f(\bar{k}) - \frac{m_0}{\hbar \tau_d} \frac{1}{4\pi^3} \int d^3 k \frac{\partial E(\bar{k})}{\partial k_x} f_0(\bar{k}).$$

(15) Evidently, the average vector velocity of electrons in equilibrium is zero:

$$\bar{V}_x = \frac{1}{\hbar} \frac{\partial E}{\partial k_x} \Big|_{\text{eq}} = \frac{1}{\hbar} \frac{\partial E}{\partial k_y} \Big|_{\text{eq}} = \frac{1}{\hbar} \frac{\partial E}{\partial k_z} \Big|_{\text{eq}} = 0.$$

Therefore,

$$\int \frac{\partial E}{\partial k_x} f_0(\bar{k}) d^3 k = 0.$$

Thus,

$$\frac{dM_x}{dt} = \frac{m_0}{\hbar\tau_d} \frac{1}{4\pi^3} \int \frac{\partial E}{\partial k_x} f(\bar{k}) d^3k. \quad (\text{C.3})$$

(16) To relate the momentum change to force, we have the current density given as

$$j_x = (-e)n\bar{V}_x = (-e) \int \frac{d^3k}{4\pi^3} f(\bar{k}) \cdot \frac{1}{\hbar} \frac{\partial E(\bar{k})}{\partial k_x}, \quad (\text{C.4})$$

where $n = \frac{d^3k}{4\pi^3} f(\bar{k})$ is the number of electrons per unit volume with \bar{k} belonging to d^3k . Indeed, $\frac{d^3k}{4\pi^3}$ is the number of “single electron cells” in the “volume” of d^3k of k -space, and $f(\bar{k})$ is the “inhabitation” of cell.

(17) Combining Eqs. (C.3) and (C.4), we obtain

$$\frac{dM_x}{dt} = -\frac{j_x m_0}{e\tau_d}. \quad (\text{C.5})$$

This is a momentum change along the x -direction, transferred to defects (the diffusing atoms) per unit time per unit volume.

(18) Let N_d be the density of defects (number of defects per unit volume). Then, according to Newton’s second law, the force at one defect, caused by electron wind, is

$$F_x = \frac{1}{N_d} \frac{dM_x}{dt} = -\frac{j_x m_0}{e\tau_d N_d}. \quad (\text{C.6})$$

This force has a clear physical meaning assuming the condition that during atomic jump the defect feels much more than one collision. Characteristic time of one successful jump is of the order of Debye time, $\tau_{\text{Debye}} \sim 10^{-13}$ sec. So for Eq. (C.6) to be reasonable, it is necessary that the product of scattering frequency, ν_{scatter} , and Debye time be much less than unity:

$$\nu_{\text{scatter}} \approx \frac{kT}{\varepsilon_p} \frac{V_F}{l}$$

where l is the mean free path length of electron around defect, V_F/l is the frequency of “possible” collisions, and kT/ε_p is the fraction of electrons which are able to be scattered according to the Pauli principle.

$l \approx \frac{1}{n\sigma}$ where σ is the cross section and is about 10^{-19} m^2 (according to Huntington’s estimate).

$$n \sim 10^{29} \text{ m}^{-3} (n_{\text{ex}} \approx \frac{kT}{\varepsilon_p} n \approx 10^{27} \text{ m}^{-3}), \frac{kT}{\varepsilon_p} \approx 10^{-2}, V_F = \frac{\hbar k_F}{m_0} \approx 10^6 \text{ m/sec}.$$

Thus, $\nu_{\text{scatter}} \approx 10^{-1}10^6 n\sigma \approx 10^{-2}10^6 10^{29}10^{-19} \approx 10^{14} \text{ sec}^{-1}$.

So $\nu_{\text{scatter}}\tau_{\text{Debye}} \approx 10 \gg 1$.

(19) Let us now transform Eq. (C.6) in terms of electric field: $j_x = \frac{\varepsilon_x}{\rho}$, where ρ is an average resistance of metal. According to the Drude–Lorentz–Sommerfeld model, the resistance ρ of a metal can be written as

$$\rho = \frac{|m^*|}{ne^2\tau},$$

where $m^* = \frac{\hbar^2}{\frac{\partial^2 E}{\partial k^2}}$ is the effective electron mass.

Huntington used the same expression for the resistance of defects,

$$\rho_d = \frac{|m^*|}{ne^2\tau_d}, \text{ so that we have } \tau_d = \frac{|m^*|}{ne^2\rho_d}.$$

Thus, from Eq. (C.6), we obtain

$$F_x = -\frac{\varepsilon_x}{\rho} \frac{m_0}{eN_d} \frac{ne^2\rho_d}{|m^*|} = -\left(\frac{m_0}{|m^*|} \frac{ZN}{N_d} \frac{\rho_d}{\rho}\right) e\varepsilon_x, \quad (\text{C.7})$$

where N is the density of ions and Z is the valence number; $n = ZN$. Thus, we have the effective charge

$$Q^* = -Z^*e, \text{ where } Z^* = \frac{m_0}{|m^*|} \frac{ZN}{N_d} \frac{\rho_d}{\rho} = Z \frac{m_0}{|m^*|} \frac{\rho_d}{N}.$$

(20) Now, let us take into account the fact that τ_d , ρ_d , and F_x change from position to position. Obviously, they shall reach a maximum at the saddle point of diffusion.

Assume that $F(y) = F_m \sin^2(\frac{\pi y}{d})$, where y is not the y -axis. Rather it is a coordinate along the jumping path, which usually does not coincide with the x -axis. Work or change of potential barrier is

$$U_j = \int_0^{a_j/2} F(y)dy = F_m \cos \theta_j \int_0^{a/2} \sin^2 \frac{\pi y}{a} dy = \frac{a_j F_m}{4} \cos \theta_j.$$

After averaging in all possible jump directions, we have

$$J_x = C \frac{D}{kT} \frac{1}{2} F_m.$$

The factor of $1/2$ is due to the integral of

$$\int_0^{a/2} \sin^2 \frac{\pi y}{a} dy = \frac{1}{2} \frac{a}{2}.$$

(21) Thus, we have finally the effective charge number:

$$Z_{\text{eff}}^* = \frac{1}{2} Z_{\text{max}}^* - Z = Z \left(\frac{1}{2} \frac{m_0}{|m^*|} \frac{\frac{\rho_d^{\text{max}}}{N_d}}{\frac{\rho}{N}} - 1 \right).$$

Subject Index

A

accelerated test of Sn whisker
 growth, 175
accelerometer, 319
Al electromigration, 212, 215, 216,
 222, 224, 225, 226, 229, 230
anisotropic conductor, 235, 238
anisotropic conducting polymer
 tapes, 31
Au/Cu/Cr under-bump
 metallization, 15, 73, 94
Au/Cu/Cu-Cr, 97, 100
Au Sn₄, 183, 198
AuSnPb ternary phase diagram, 199

B

back stress, 222, 225
back stress build-up, 228
back stress measurement, 229
back stress of electromigration, 222,
 226
ball-grid array (BGA) solder balls, 16
ball-limiting metallization (BLM), 15
Burger's equation, 286
beta-Sn (β -Sn), 153, 235
ball-grid array (BGA) board, 315
Blech structure, 212, 228, 231
bond pad, 9, 23, 24
bronze, 1
bulk diffusion couple of SnPb, 123

C

C-4 flip chip technology, 12
Coble creep model, 160

cakine, 115
Charpy impact test, 311, 314
channel between scallops, 128, 150
chemical potential, 90, 170, 224
chip-packaging interaction, 30, 124
chip-size packaging, 29
cold joint, 7, 183, 198
composite solder joint, 20, 113, 272,
 310, 329
compressive stress gradient, 16, 153,
 160, 163
constant volume constraint, 283, 343
consumption rate of Cu, 48, 69
continuity equation, 173
controlled-collapse-chip-connection
 (C-4) solder joint, 14, 97
Coffin-Manson mode of low cycle
 fatigue, 22
copper-tin binary system, 1
copper-tin reaction, 3, 37, 73, 111,
 127, 154
creep, 16, 74, 154, 325, 345
critical length of electromigration,
 223, 225
critical product of electromigration,
 224, 247
(Cu, Ni)₆ Sn₅, 102, 104, 193
Cu/Ni(V)/Al under-bump
 metallization, 73, 100, 251, 273,
 275, 329, 335
Cu/Sn room temperature reaction,
 74
Cu-solder-Cu samples for tensile
 test, 306

Cu column bump, 276
CuSnPb ternary phase diagram, 56
Cu₃ Sn, crystal structure, 45, 75, 78
Cu₆ Sn₅, crystal structure, 44, 75
Cu₆ Sn₅, crystallographic orientation, 43, 45
Cu₆ Sn₅, growth kinetics, 75, 80
Cu₆ Sn₅, sequential formation, 81
current crowding, 230, 247, 250
current density gradient force, 230

D

daisy chain of flip chip solder joint, 253
Darken's analysis of interdiffusion, 157, 227
deformation potential, 225
deviatoric strain, 166
dewetting, 96
diffusion barrier, 178, 280
diffusion controlled reaction (or growth), 63, 84
dilatation strain, 166
direct chip attachment, 17
direct force of electromigration, 218
drift velocity, 212, 220
drop test, 316
dual damascene structure, 214
ductile-to-brittle transition in solder joint, 25, 306
ductile-to-brittle transition temperature (DBTT), 312
dynamic equilibrium, 299

E

effective charge number of electromigration, 220, 257, 364
electroless Ni(P) UBM, 19, 188
electromigration, 25, 119, 176, 212, 245
electromigration in eutectic solder joint, 249, 255
electron wind force of electromigration, 217
eutectic effect of phase separation, 119
eutectic SnAgCu, 6, 67
eutectic SnAg, 6, 67
eutectic SnCu, 6, 67

eutectic two-phase structure, 119, 281

F

facetted scallop, 53, 143, 15
flexional vibration, 322
flux divergence, 216
flip chip solder joint, 111, 245
flip chip technology, 12
focused ion beam thinning, 172
free energy of formation of vacancy, 89, 350
free energy of motion of vacancy, 89, 348
frequency of vibration, 319

G

glancing incidence x-ray diffraction, 74
gradient of chemical potential, 112, 119
gradient of current density, 234
gradient of volume fraction, 112, 119, 282
grain boundary precipitation, 156, 158, 179

H

halo formation, 42
high speed shear, 314, 316
hillock, 155, 292
homogenization, 120, 327
homologous temperature, 215, 228, 305

I

intermetallic compound (IMC), 17, 38, 60, 62, 69, 73, 128, 131, 158, 183, 194, 198, 293, 296, 298, 301
immersion Sn, 11
impact fracture, 25, 316
input/output (I/O) pads, 12
interconnect, 214
interdiffusion coefficient, 62, 87
interfacial reaction coefficient, 89
interfacial reaction-controlled reaction, 62, 87, 89
interfacial tension of SnPb alloy, 51
interstitial diffusion, 74, 117

J

JEDEC-JESP22-B111 standard of drop test, 316
 JEDEC specification of drop test, 312, 316
 joule heating, 26, 211, 254, 270

K

Kirkendall effect of interdiffusion, 159
 Kirkendall shift, 159, 285
 Kirkendall void, 59, 101, 192, 279, 295

L

lamellar microstructure, 112, 119, 281
 Laue pattern, 164
 layer-type (layered) morphology, 61, 84, 88, 131, 133
 leadframe, 9, 16, 153
 line-to-bump geometry, 26, 246, 249
 low cycle fatigue, 1, 22
 LSW theory of conservative ripening, 137, 148

M

marker displacement, 80, 262, 263
 matte Sn, 17, 153
 mean-time-to-failure (MTTF), 245, 264
 mini Charpy machine, 314
 miniaturization, 28
 Moire interferometry, 124
 mono-size distribution, 135, 137
 monochromator, 167
 morphological stability of scallops, 128
 multi-chip module, 14
 multi-level metal-ceramic module, 14

N

Nabarro-Herring creep model, 160
 near-ideal flip-chip solder joint, 280
 NEMI (National Electronics Manufacturing Initiative), 178
 NiSnPb ternary phase diagram, 185
 Ni₃P, 188, 192
 Ni₃Sn₄, 184, 188

(Ni, Cu)₃Sn₄, 193
 non-conservative ripening, 128, 139

O

Onsager's reciprocity relations, 170, 225
 over-hang, 232

P

pancake-type void, 245, 253, 254, 267
 Pb-free solder, 4, 38, 68
 PdSnPb ternary phase diagram, 197
 phased-in Cu-Cr UBM, 14, 97
 phase separation, 121, 248, 281, 333
 pin-through-hole technology, 10, 12
 polarity effect, 289
 polarity effect on IMC growth, 293, 297, 301

R

random phase distribution, 282, 286, 334
 random state, 282, 334
 reflow, 2, 15
 reliability of solder joint technology, 16
 ripening, 41, 64, 139
 RMA (mildly activated rosin flux), 38
 Rutherford backscattering spectrum (RBS), 77, 83

S

scallop, 40, 41, 43, 53, 64, 68, 93, 127, 131, 1
 scallop-type morphology, 131
 Seeman-Bohlin x-ray diffractometer, 74, 92
 silicide, 82, 129
 single-phase growth, 82, 129
 SIP (system-in-packaging), 29
 size distribution function, 141, 148
 Sn whisker, 16, 153
 SOP (system-on-packaging), 29
 SOC (system-on-chip), 29
 solder finish, 153
 solder-less joint, 31
 solder bumping, 114
 solder cap, 39

solder fountain, 10
Soret effect, 119, 327, 343
spalling, 17, 93, 100, 101, 104, 117
spontaneous Sn whisker growth,
153
surface mount technology, 12, 153
stochastic behavior, 343
stochastic tendency, 286
synchrotron radiation, x-ray
micro-diffraction, 43, 163

T

temperature gradient, 327
theory of non-conservative ripening,
139
thermal mechanical stress, 22, 30,
124
thermal mismatch, 2
thermomigration, 25, 327
thermomigration in eutectic
two-phase alloy, 329, 343
thermomigration in SnPb solder,
335
thermomigration, fundamentals,
338
thin-film under-bump-metallization,
111
time-dependent melting, 270
torque, 237, 320
two level packaging, 14

U

ultra-low k materials, 30
under-bump metallization (UBM),
14, 60, 7
underfill, 1, 23, 30

V

v-groove, 105, 289, 306
very-large-scale-integration (VLSI),
12, 211

W

wear-out failure of electromigration,
232
wetting angle, 38, 40, 49, 50
wetting reaction, 2, 3, 38
wetting reaction as a function of
SnPb composition, 48
wetting tip, 43, 105
Wiedemann-Franz law, 271
wire bonding, 9, 12

X

x-ray micro-diffraction, 229

Y

Young's equation, 49

Z

zincated Al surface, 188

Springer Series in
MATERIALS SCIENCE

Editors: R. Hull R.M. Osgood, Jr. J. Parisi H. Warlimont

- 30 **Process Technology for Semiconductor Lasers**
Crystal Growth and Microprocesses
By K. Iga and S. Kinoshita
- 31 **Nanostructures and Quantum Effects**
By H. Sakaki and H. Noge
- 32 **Nitride Semiconductors and Devices**
By H. Morkoç
- 33 **Supercarbon**
Synthesis, Properties and Applications
Editors: S. Yoshimura and R. P. H. Chang
- 34 **Computational Materials Design**
Editor: T. Saito
- 35 **Macromolecular Science and Engineering**
New Aspects
Editor: Y. Tanabe
- 36 **Ceramics**
Mechanical Properties,
Failure Behaviour,
Materials Selection
By D. Munz and T. Fett
- 37 **Technology and Applications of Amorphous Silicon**
Editor: R. A. Street
- 38 **Fullerene Polymers and Fullerene Polymer Composites**
Editors: P. C. Eklund and A. M. Rao
- 39 **Semiconducting Silicides**
Editor: V. E. Borisenko
- 40 **Reference Materials in Analytical Chemistry**
A Guide for Selection and Use
Editor: A. Zschunke
- 41 **Organic Electronic Materials**
Conjugated Polymers and Low Molecular Weight Organic Solids
Editors: R. Farchioni and G. Grosso
- 42 **Raman Scattering in Materials Science**
Editors: W. H. Weber and R. Merlin
- 43 **The Atomistic Nature of Crystal Growth**
By B. Mutafschiev
- 44 **Thermodynamic Basis of Crystal Growth**
 P - T - X Phase Equilibrium and Non-Stoichiometry
By J. Greenberg
- 45 **Thermoelectrics**
Basic Principles and New Materials Developments
By G. S. Nolas, J. Sharp, and H. J. Goldsmid
- 46 **Fundamental Aspects of Silicon Oxidation**
Editor: Y. J. Chabal
- 47 **Disorder and Order in Strongly Nonstoichiometric Compounds**
Transition Metal Carbides, Nitrides and Oxides
By A. I. Gusev, A. A. Rempel, and A. J. Magerl
- 48 **The Glass Transition**
Relaxation Dynamics in Liquids and Disordered Materials
By E. Donth
- 49 **Alkali Halides**
A Handbook of Physical Properties
By D. B. Sirdeshmukh, L. Sirdeshmukh, and K. G. Subhadra
- 50 **High-Resolution Imaging and Spectrometry of Materials**
Editors: F. Ernst and M. Rühle
- 51 **Point Defects in Semiconductors and Insulators**
Determination of Atomic and Electronic Structure from Paramagnetic Hyperfine Interactions
By J.-M. Spaeth and H. Overhof
- 52 **Polymer Films with Embedded Metal Nanoparticles**
By A. Heilmann
-

Springer Series in
MATERIALS SCIENCE

Editors: R. Hull R.M. Osgood, Jr. J. Parisi H. Warlimont

- 53 **Nanocrystalline Ceramics**
Synthesis and Structure
By M. Winterer
- 54 **Electronic Structure and Magnetism of Complex Materials**
Editors: D.J. Singh and D. A. Papaconstantopoulos
- 55 **Quasicrystals**
An Introduction to Structure, Physical Properties and Applications
Editors: J.-B. Suck, M. Schreiber, and P.Häussler
- 56 **SiO₂ in Si Microdevices**
By M. Itsumi
- 57 **Radiation Effects in Advanced Semiconductor Materials and Devices**
By C. Claeys and E. Simoen
- 58 **Functional Thin Films and Functional Materials**
New Concepts and Technologies
Editor: D. Shi
- 59 **Dielectric Properties of Porous Media**
By S.O. Gladkov
- 60 **Organic Photovoltaics**
Concepts and Realization
Editors: C. Brabec, V. Dyakonov, J. Parisi and N. Sariciftci
- 61 **Fatigue in Ferroelectric Ceramics and Related Issues**
By D.C. Lupascu
- 62 **Epitaxy**
Physical Principles and Technical Implementation
By M.A. Herman, W. Richter, and H. Sitter
- 63 **Fundamentals of Ion-Irradiated Polymers**
By D. Fink
- 64 **Morphology Control of Materials and Nanoparticles**
Advanced Materials Processing and Characterization
Editors: Y. Waseda and A. Muramatsu
- 65 **Transport Processes in Ion-Irradiated Polymers**
By D. Fink
- 66 **Multiphased Ceramic Materials**
Processing and Potential
Editors: W.-H. Tuan and J.-K. Guo
- 67 **Nondestructive Materials Characterization**
With Applications to Aerospace Materials
Editors: N.G.H. Meyendorf, P.B. Nagy, and S.I. Rokhlin
- 68 **Diffraction Analysis of the Microstructure of Materials**
Editors: E.J. Mittemeijer and P. Scardi
- 69 **Chemical-Mechanical Planarization of Semiconductor Materials**
Editor: M.R. Oliver
- 70 **Applications of the Isotopic Effect in Solids**
By V.G. Plekhanov
- 71 **Dissipative Phenomena in Condensed Matter**
Some Applications
By S. Dattagupta and S. Puri
- 72 **Predictive Simulation of Semiconductor Processing**
Status and Challenges
Editors: J. Dabrowski and E.R. Weber
- 73 **SiC Power Materials**
Devices and Applications
Editor: Z.C. Feng
- 74 **Plastic Deformation in Nanocrystalline Materials**
By M.Yu. Gutkin and I.A. Ovid'ko
- 75 **Wafer Bonding**
Applications and Technology
Editors: M. Alexe and U. Gösele
- 76 **Spirally Anisotropic Composites**
By G.E. Freger, V.N. Kestelman, and D.G. Freger
- 77 **Impurities Confined in Quantum Structures**
By P.O. Holtz and Q.X. Zhao
-